

Original article

A numerical analysis of background flow velocity effects on long-term post-injection migration of CO₂ plumes in tilted storage aquifers

Mawda Awag^{✉*}, Eric Mackay, Saeed Ghanbari

Institute of GeoEnergy Engineering, Heriot-Watt University, Edinburgh EH14 4AS, United Kingdom

Keywords:

CO₂ plume migration
background flow velocity
tilted aquifer
plume distribution
plume instantaneous velocity

Cited as:

Awag, M., Mackay, E., Ghanbari, S. A numerical analysis of background flow velocity effects on long-term post-injection migration of CO₂ plumes in tilted storage aquifers. *Advances in Geo-Energy Research*, 2024, 11(2): 103-114.

<https://doi.org/10.46690/ager.2024.02.03>

Abstract:

Even though groundwater flow exists in many saline aquifers, very few studies have investigated its significance on the injected CO₂ migration and trapping processes. Here, a numerical simulation approach is used to study the late post-injection migration and trapping of CO₂ injected into a tilted aquifer. The analysis highlights that although the migration of the CO₂ and its dissolution in brine is induced by buoyancy, the existence of background flow can further affect the plume velocity, convective dissolution, the dissolved CO₂ flux and its distribution in the storage complex. Our analysis shows that the background flow removes the residual CO₂, by dissolution, before the convective dissolution of the mobile part becomes dominant. The plume decelerates during its vertical migration by a factor of 6.5; then, its height increases with time to more than 15% as background flow velocity increases, hence reducing its rate of deceleration. However, when the plume reaches its maximum height, it migrates with a constant velocity. Greater background flow velocity not only allows the plume to migrate further, but it may hinder CO₂ dissolution. This is because it can transport the dissolved CO₂ underneath the plume for a long time, thus slowing down the interaction at the CO₂-brine interface. The weak and strong background flows can impact the tendency of the dissolved CO₂ to persist underneath the caprock. Our results indicate the existence of a critical background flow velocity which can control the distribution of the dissolved CO₂ at the bottom of the aquifer, further away from the caprock.

1. Introduction

To date, deep saline aquifers are the most widely used geological formations for long-term and secure storage of carbon dioxide (CO₂) (Birkholzer et al., 2015). Typically, saline aquifers located at depths of 1 to 3 km under the surface are used (MacMinn et al., 2010). Pilot scale sites for CO₂ storage (e.g., Alberta basin in Canada, Frio formation in Texas, Ketzin site in Germany, Carrizo-Wilcox aquifer in the Texas, and Ordos carbon capture and storage site in China) are rarely located in horizontal strata, and instead have slight to significant degrees of tilt (ranging from less than 1° to more than 15°) (Bachu et al., 1994; Förster et al., 2006; Hovorka et al., 2006; Nicot, 2008; Pruess and Nordbotten, 2011; Wang

et al., 2016; Han and Kim, 2018). In addition, aquifers are usually exposed to groundwater flow. Such as, the Alberta Basin with groundwater velocities ranging between 0.01-0.10 m/year (Han et al., 2011). A greater capacity for CO₂ storage exists in saline aquifers that are tilted to a significant degree (Pruess and Nordbotten, 2011) rather than shallow dipping or horizontal systems. The injected CO₂ is buoyant with respect to the resident aquifer brine due to the density contrast; however, its migration can be further driven by the background water flow of the aquifer and/or the degree of dip of the formation strata (Elenius et al., 2015). Furthermore, the potential for CO₂ displacement out of the storage complex is increased if the migrating plume encounters a spill point feature (Emami-Meybodi et al., 2015). Consequently, ensuring

the CO₂ becomes immobilised and remains within the storage formation is crucial for storage security.

The injected CO₂ is retarded by different trapping processes that act over different timescales. The plume of injected CO₂ is retained in underground via an impermeable caprock, which forms the structural trapping (Bachu et al., 1994). Then, some of the CO₂ is immobilised by capillary forces at the trailing edges of the migrating plume, forming residually trapped CO₂ (Kumar et al., 2005; Juanes et al., 2009; Pruess and Nordbotten, 2011). Over time, the entire CO₂ plume will dissolve gradually into the aquifer water to cause solubility trapping. The dissolved CO₂ develops a diffusive layer of CO₂-rich brine that is denser than that of the aquifer brine, which expands with time and causes gravitational instabilities. The CO₂-rich brine sinks to the bottom of the storage complex, allowing unsaturated brine to interact with more of the CO₂, initiating the convective mixing process and additional CO₂ dissolution (Emami-Meybodi et al., 2015). Solubility trapping is a safe and effective means of containing CO₂ (Emami-Meybodi et al., 2015). With this mechanism, CO₂ is trapped as a soluble component in the formation brine and is considered immobile as long as the host formation brine remains immobile (Mackay, 2013; Riaz and Cinar, 2014). However, in cases where the brine is mobile, e.g., if there is groundwater flow or water injection or production to maintain pressure, the dissolved CO₂ may migrate over large distances within the porous medium (Nghiem et al., 2010). Over a very long timescale, the most secure form of trapping occurs when the dissolved CO₂ reacts with the rock minerals and converts them into carbonate minerals (Gunter et al., 1997; Oh et al., 2017). However, CO₂ mineralisation reactions can take hundreds and even thousands of years to contribute because of the slow reaction dynamics, which do not impact the plume migration (Nghiem et al., 2010).

The injected CO₂ plume will continue to migrate in the subsurface after cessation of injection for a long period of time, before it becomes completely immobilised by the different trapping processes (Bachu, 2015). Analysing and modelling the post-injection distribution of the injected CO₂ and its partitioning in the aqueous phase is crucial to assess the integrity of the long-term CO₂ storage in the aquifer. Different analytical and numerical studies investigated CO₂ storage in open dipping storage aquifers, but not many considered the displacement of aquifer water. Amongst previous studies, Pruess and Nordbotten (2011) investigated with numerical simulations long-term CO₂ migration in a slightly tilted aquifer, considering a non-hysteretic effect in the relative permeability and capillary pressure models, and accounted for the dissolution of CO₂ in brine. Their analysis showed that the injected CO₂ migrates with a uniform velocity irrespective of the degree of dip angle of the aquifer, because the front has an unchanging saturation, relative permeability and mobility. Similarly, Wang et al. (2016) studied long-term plume migration, including the injection period, while neglecting the impact of hysteresis but considering CO₂ dissolution. They found that during the post-injection, the plume migrates a greater distance, indicating that the effect of the dipping of the strata is significant in assessing the storage efficiency.

Most recently, Han and Kim (2018) considered the effect of both relative permeability hysteresis and capillary pressure in their modelling to analyse the plume migration under dipping sinusoidal caprock structures. They indicated that the velocity of the plume is most sensitive to the dip angle of the aquifer.

Other researchers analysed the role of brine injection and production in increasing CO₂ trapping in the storage formation. Leonenko and Keith (2008) investigated the impact of brine injection on the CO₂ solubility process. They carried out a numerical study involving CO₂ injection through a horizontal well into an aquifer, brine injection using the same horizontal well after CO₂ injection stops, and brine production using wells placed far enough away to prevent breakthrough. Their study indicated a stronger convective mixing with brine injection and an acceleration in dissolution. Cameron and Durlofsky (2012) also analysed the application of produced brine in enhancing the solubility trapping of the CO₂ and the residual CO₂ trapping. They modelled water production from the deepest point in the aquifer and its immediate reinjection into the top of the aquifer. They found that brine injection can have a great influence on the mobile CO₂ plume. However, their simulations do not include the impact of water flow on the density-driven instabilities caused by convective dissolution and the velocity of the evolving plume.

Few other studies have taken into consideration the existence of background water in aquifers. Hassanzadeh et al. (2009) introduced a numerical approach to model an increase in CO₂ dissolution through injecting brine over an injected CO₂ in a saline aquifer. They suggested that dissolution can be enhanced by brine injection, resulting in more than 50% of the injected buoyant plume being stored through solubility trapping. In another study, Hassanzadeh et al. (2009) presented a linear stability analysis of the effect of groundwater flow and dispersion on the onset of convection for several Alberta basin aquifers. They established that the existence of groundwater flow in saline aquifers can postpone the beginning of convection, resulting in a longer dissolution timescale. Similarly, Emami-Meybodi et al. (2015) developed a semi-analytical model to study the role of groundwater flow in aquifers on CO₂ dissolution in brine. Then, with numerical analysis, they analysed the behavior of convective mixing during the dissolution process. Their study showed that the background flow can retard the onset of free convection and consequently the subsequent mixing between the CO₂ and brine. Meanwhile, Michel-Meyer et al. (2017) carried out an experimental study using a methanol and ethylene-glycol mixture as an analogue for CO₂ to analyse the impact of horizontal water flow on the CO₂ dissolution process. They found that the imposed background water flow does not impact the rate of dissolution, but it suppresses the formation of fingers that are developed by convective mixing.

In our previous study (Awag et al., 2023), the influence of the magnitude of groundwater on the advancement of the CO₂ is analysed throughout the early post-injection stage, considering the significance of the residual trapping and the CO₂ dissolution in water on the plume advancement. The analysis suggests that mobile CO₂ reduces at larger background flow velocities. However, increasing the background flow allows

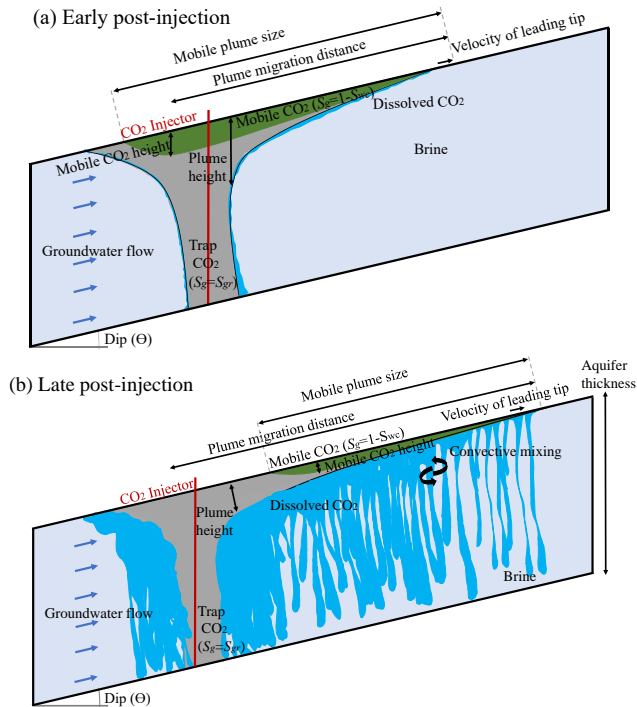


Fig. 1. the migration of a plume of CO₂ in a conceptual dipping aquifer system with updip groundwater flux during the early and late post-injection periods. Region 1 comprises mobile CO₂ and a connate water saturation S_{wc} (green); Region 2 contains the residual CO₂ S_{gr} and mobile water (grey); Region 3 indicates the dissolved CO₂ in water (blue). (a) Early post-injection and (b) Late post-injection.

the CO₂ to advance further and accelerate during its early lateral migration. In a different study (Awag et al., 2024a), the influence of the direction and magnitude of groundwater on the evolution of CO₂ in aquifer was analysed during the post-injection period. Recently, Awag et al. (2024b) compared the CO₂ plume migration at various dipping aquifers when the direction of aquifer water is downdip with that when it is in the updip. It was concluded from both studies that the downdip flow extends the plume extent further and causes it to migrate with greater velocity due to increasing the buoyancy than the updip flow, thus increasing the CO₂ leakage potential.

In order to build on the knowledge gained from the aforementioned works, our objective in this study is to understand the role of groundwater flow on, specifically, the velocity of the injected CO₂ throughout the late post-injection time, considering the interaction of the convective mixing of the CO₂ in brine with the evolving CO₂ plume. The study shows that background flow velocity can impact the evolution of the injected plume and its lifetime in the subsurface, the dissolved CO₂ flow and the ultimate fate of CO₂.

This paper is organized as follows. First the conceptual aquifer developed for this study is introduced. Then, the methodology used is described. After that, the numerical analysis results are discussed; afterwards the conclusions drawn

from the findings of this work.

2. Model construction

2.1 Conceptual model setup

The aquifer established for this analysis is presented in Fig. 1. In this conceptual study, the CO₂ (green) is injected via a vertical injector (red), in a supercritical state, into a dipping aquifer with updip groundwater flow (from the left to the right direction). The schematic illustration captures the CO₂ post-injection evolution and trapping processes. The post-injection duration is identified at: early and late post-injection periods.

Once injection ceases, the plume of injected CO₂ replaces the resident brine at its leading tip (in a drainage process) and migrates vertically upwards towards the caprock due to phase density differences. Residual CO₂ forms at the trailing edges of the migrating CO₂ due to water displacement during the imbibition process (the grey section in the diagram). The injected CO₂ gradually dissolves into the underlying brine developing a dissolved boundary layer at the CO₂-brine interface (the blue region) that is denser than the resident brine. As discussed in our previous study (Awag et al., 2023), during the early post-injection period, the dissolved front at the leading edges of the migrating plume (the blue region across the interface between the mobile CO₂ region (green) and brine in Fig. 1(a)) is not yet thick enough to fall to the bottom of the aquifer.

On the other hand, during the late post-injection period, the thickness of the dissolved CO₂ layer increases with time and sinks downwards, allowing fresh brine to interact with more CO₂ at the CO₂-brine interface. This in turn forms descending plumes of dissolved CO₂, initiating convective mixing patterns (circulation arrows in Fig. 1(b)). The convective dissolution of CO₂ gradually consumes all the mobile and residually trapped CO₂, immobilising the CO₂ and bringing its advancement to an end. Depending on the aquifer conditions, the fate of the CO₂ will either secure the dissolved CO₂ at the bottom boundary of the storage domain, or it will be affected by the brine displacement.

The study here highlights the influence of the magnitude of groundwater, during the late post-injection period, on the migration pattern and the velocity of the CO₂ plume, the amount of residually trapped CO₂ and convective dissolution of CO₂ in brine, and the fate of CO₂.

2.2 Numerical simulation model

A two-dimensional dipping storage aquifer is developed to run using the Computer Modelling Group GEM reactive transport reservoir simulator (a multi-dimensional, finite-difference, three-phase and compositional model) (CMG-GEM, 2022). The simulator is used to isothermally model the conceptual system shown in Fig. 1. Fig. 2 displays the aquifer system used for this study to explore the effect of the magnitude of groundwater on the migration and inventory of the injected CO₂. The size of the aquifer domain is 20 km in the X dire-

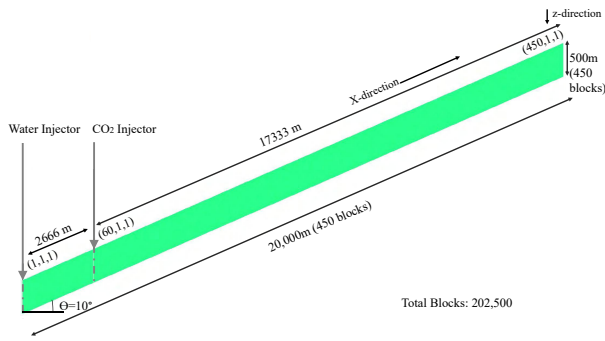


Fig. 2. Illustration of the 2D dipping aquifer storage model.

Table 1. Aquifer model properties.

Model parameters	Value
Total pore volume (m^3)	1.3×10^{10}
Porosity (%)	13
Horizontal permeability K_h (mD)	97.5
Permeability anisotropy ratio (K_v/K_h)	1
Aquifer dip angle ($^\circ$)	10
Reference depth to the top of injector (m)	4,650
Initial reservoir pressure (kPa)	49,000
Reservoir temperature ($^\circ C$)	200
Corey exponent for gas	1.8
Corey exponent for water	2.3

ction and 0.5 km in the Z direction, which is large enough to predict the post-injection CO₂ plume evolution before reaching the aquifer edge boundaries. The domain is discretized into 450 × 450 cells in the X- and Z-directions. This discretization gives an acceptable compromise between grid resolution and computational run time, which also allows the thin plume underneath the caprock to be precisely located, and to obtain the plume migration and dissolution patterns. The grid is homogeneous and isotropic in permeability and homogenous in porosity; this choice is made to isolate the contribution of groundwater flow velocity from the influence of the heterogeneities on the injected CO₂ migration velocity and trapping. Additional pore volume is added to the vertical boundary the model on its updip side (that is right in Fig. 2, from grid block 450 in the X-direction to grid block 450 in the Z-direction), indicating a further areal extent of the aquifer, to prevent pressure buildup in the model. (This was achieved by multiplying the pore volume in the cells in the 450th column on the right hand side of the model by a factor of 1,010). Table 1 presents the aquifer parameters used in this modelling.

An isothermal two-phase system is considered in this study, which contains CO₂ as a supercritical phase and water as an aqueous phase (including that with dissolved CO₂). The Jossi et al. (1962) correlations and the Peng and Robinson (1976) Equation of State are used to compute the density and viscosity of the supercritical CO₂, respectively. While correlations of

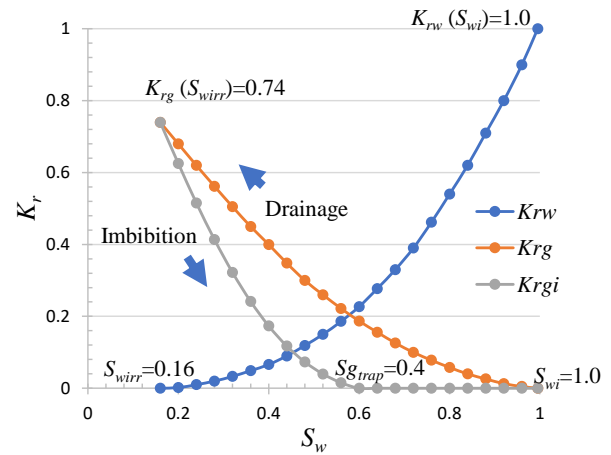


Fig. 3. The relative permeability functions.

Rowe and Chou (1970) and Kestin et al. (1981) are used to determine the density and viscosity of the aqueous phase at the reservoir conditions, respectively. The geomechanical stresses or geochemical reactions and evaporation of water into the supercritical phase are not included in this study. However, Henry's law (Li and Nghiem, 1986; Harvey, 1996) is included in the modelling study to model the CO₂ solubility in water.

Fig. 3 shows the relative permeability data applied in this numerical analysis. Relative permeability hysteresis of the gas phase is considered in the model with a residual CO₂ $S_{gr} = 0.40$. Land (1968) correlation is used to determine the imbibition curves. Capillary pressure is not modelled, as its impact is beyond the scope of this study, but it will be studied in a future analysis.

The aquifer domain has a vertical CO₂ injection well, at grid block 60 in the I-direction in Fig. 2, that fully penetrates the whole thickness of the aquifer. In all sensitivity models, CO₂ is injected, at reservoir condition, during a one-year period with a total injection of 2.5% PV/year that is constant in time. The injection time and rate are chosen to maintain the CO₂ long enough inside the storage throughout the total duration of the simulation runtime. This is a realistic rate which in this conceptual study allows for proper comparisons of the findings. However, CO₂ can be injected at varied rates for extended periods. In this study, a timeline of observation for the plume migration and trapping during late post-injection time is considered for 1,000 years.

The aquifer's top and bottom boundaries consider no flow boundary conditions. In addition, a vertical water injection well is incorporated into the sensitivity models and is perforated thru the complete interval, to emulate groundwater displacement across the aquifer. The water injector is located on the downdip boundary (that is left in Fig. 2, at grid block 1 in the X-direction). The groundwater in aquifers moves at a relatively slow velocity (typically less than 1 km/yr) compared to that of pumped fluids (Harter, 2003). In this study, it is assumed that the groundwater flows at a moderate velocity of $1 U_w = 0.003048$ m/day. This is varied in the simulation scenarios at different ratios between 0 to 15 U_w , in order to analyse its effect on the plume migration.

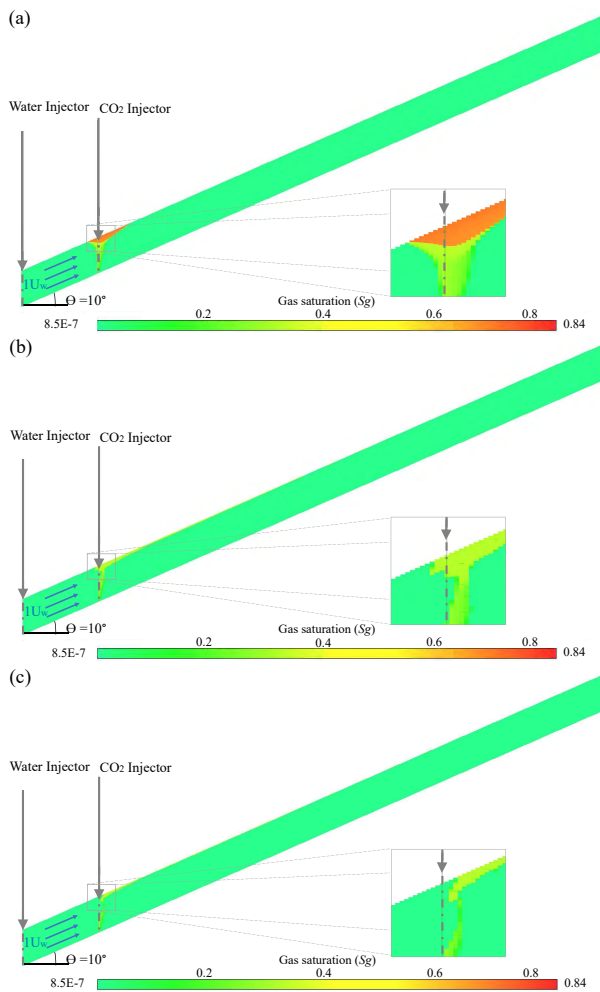


Fig. 4. Plume evolution profile after (a) injection is stopped, (b) 40 years and (c) 80 years of migration for groundwater velocity of $1 U_w = 0.003048$ m/d. The red and yellow colours indicate the mobile and immobile sections of the plume, respectively.

Various sensitivity analyses are accomplished to study the impact of groundwater velocity on the migration velocity of the CO_2 and trapping mechanisms during the late post-injection period. The numerical results of this study are processed by a spreadsheet script with macro to give the accurate spreading of the plume that is measured at precise timesteps. Threshold values of gas saturation ($S_g = 0.005$) and relative permeability ($K_{rg} = 0.01$) are applied one at a time to the script, to determine the size of the total injected CO_2 and the mobile section of the plume, respectively.

3. Results

In this study, the impact of background flow velocity is considered in addition to the role of CO_2 dissolution in water on the evolution and trapping of the CO_2 throughout the late post-injection phase. Figs. 4 and 5 show the simulated distribution of the CO_2 injected into a dipping aquifer immediately after injection stops, and after 40 and 80 years, for water velocities of 1 and $15 U_w$, respectively. The shape of the plume varies dramatically with time during its late post-injection mi-

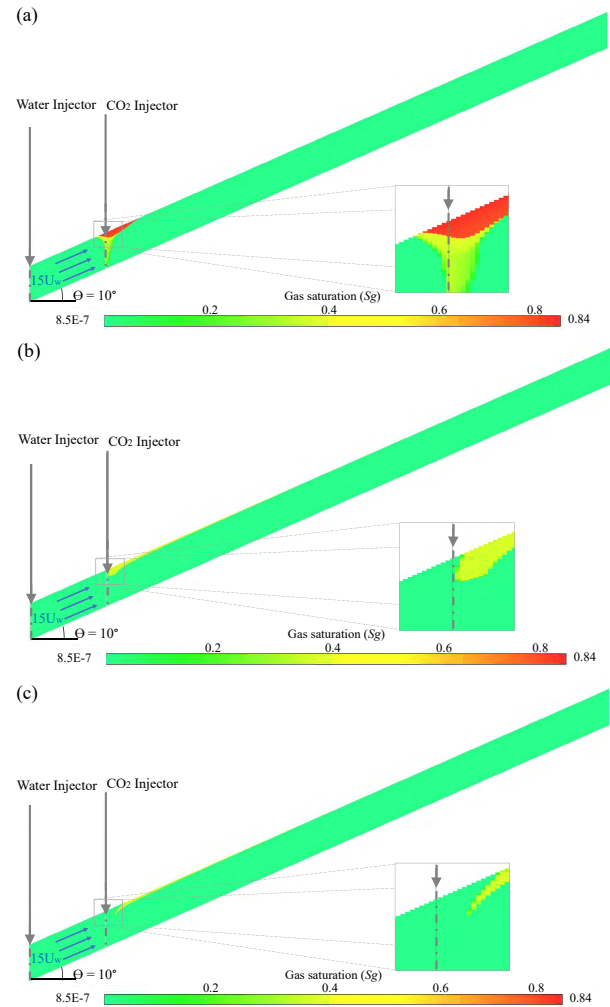


Fig. 5. Same situation as in Fig. 4 but at greater background water of $15 U_w$ (0.04572 m/d), after (a) injection is stopped, (b) 40 years and (c) 80 years of migration.

gration, especially around the injection well. It has previously been shown that during the early migration of the CO_2 the total height of the plume decreases slowly (Awag et al., 2022). By contrast, in this study, the mobile CO_2 has almost vanished throughout the late post-injection period (red region in Figs. 4 and 5). This is due to the strong impact of reservoir processes in trapping the mobile CO_2 : the residual trapping of the CO_2 at the trailing edge of the plume during water re-imbibition (the yellow parts of the plume in Figs. 4 and 5) and CO_2 dissolution in unsaturated water as the plume migrates.

In addition, comparison of Figs. 4 and 5 shows that the distribution of residually trapped CO_2 changes with background flow. The larger the background flow, the more that residual CO_2 dissolves in water, especially at the trailing edge. (This can be identified from the reduction in the yellow region). However, the dissolution of the residual CO_2 is a very slow process-slower even than dissolution of mobile CO_2 . This is due to the reduced mobility of water in the region of trapped CO_2 compared with that of the fully-saturated water region.

In order to understand how the background flow influences the long-term CO_2 dissolution process, Fig. 6 illustrates CO_2

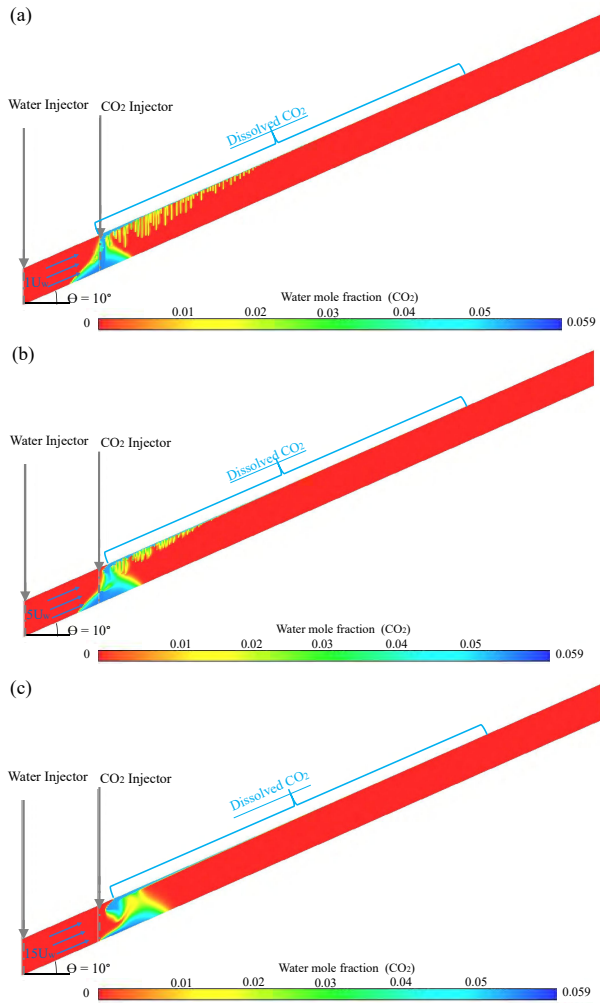


Fig. 6. Snapshots of CO₂ dissolution profiles after 80 years, for water flow velocities of (a) 1 Uw, (b) 5 Uw and (c) 15 Uw.

plume dissolution in water after 80 years, for water velocities of 1, 5 and 15 Uw. During the late migration of the CO₂ plume, the free phase CO₂ (the blue regions in Fig. 6) interacts with the mobile water and immobile residual water at the CO₂-water interface, and dissolves slowly. The zone containing a mixture of CO₂ and water then develops, producing a diffusive CO₂-saturated layer of water, denser than the underlying water (the red region in Fig. 6). The CO₂-water layer becomes unstable with time, forming vertically evolving finger patterns (the yellow/green parts in Fig. 6), initiating the convective mixing of the buoyant CO₂ and unsaturated water. However, the formation of fingers and the instabilities are suppressed by the background water flow. As the background flow velocity increases, the extent of the fingers reduces, while their width increases, which is in agreement with the experimental analysis presented by Michel-Meyer et al. (2017) and the analytical study provided by Emami-Meybodi et al. (2015).

In the slow groundwater case (1 Uw), Fig. 6(a), the fingers

formed are thinner and longer in length compared with the intermediate water flow velocity (5 Uw), Fig. 6(b). At greater background flow velocity (15 Uw), Fig. 6(c), the dissolved CO₂ creates a thick CO₂-saturated water layer with one finger (at the down-dip area of the plume), and no other fingers develop. This is because, as suggested by Emami-Meybodi et al. (2015), the horizontal flow of water can prevent the diffusive boundary layer from growing in the vertical direction and delay the onset of free convection. Hence, at high flow velocities, the convective mixing regime may not develop.

These numerical results show that the background water can impact not only the evolution of the injected CO₂, but also the residual and dissolution trapping of CO₂ during its late migration, and the ultimate fate of CO₂ in the aquifer. To gain deeper insights into the previously described results, we consider the impact of the background water on the evolution of, first, the injected CO₂ (both trapped and mobile), and then, secondly, only the mobile area of the plume. After that, the significance the water flow has on the migration velocity of the plume and the eventual fate of the plume is assessed.

3.1 Background water impact on the CO₂ plume evolution

In order to understand the overall plume behaviour, the impact of background water velocity on the advancement of the total injected volume of CO₂ (mobile and residual) is analysed over a long time period (the red and yellow sections of the plume presented in Figs. 4 and 5 above, respectively). Fig. 7 shows the change in the plume distribution for various groundwater velocities after 40, 80 and 120 years. These results were determined by the post-processing explained above. The height of the injected CO₂ decreased with increasing the background flow and with time, while its up-dip migration increased with time.

3.2 Background water effect on the migration of the mobile CO₂

The migration of the mobile portion of the plume (the red part of the plume shown in Figs. 4 and 5) is also considered with respect to the background flow velocity. Fig. 8 displays the mobile CO₂ distribution at various flow velocities, again after 40, 80 and 120 years of simulation. Fig. 9 gives the estimated size of the mobile CO₂ at various water velocities and times based on Fig. 8. A non-monotonic behaviour affects the distribution and size of the mobile CO₂, which is rather significant at low water flow velocities.

3.3 Instantaneous velocity of the plume leading tip and height of the plume at deepest point

A detailed evaluation of the long-term velocity of the plume tip is also important when investigating the role of groundwater flow on the evolving plume. Fig. 10 illustrates the plume velocity throughout the late post-injection migration

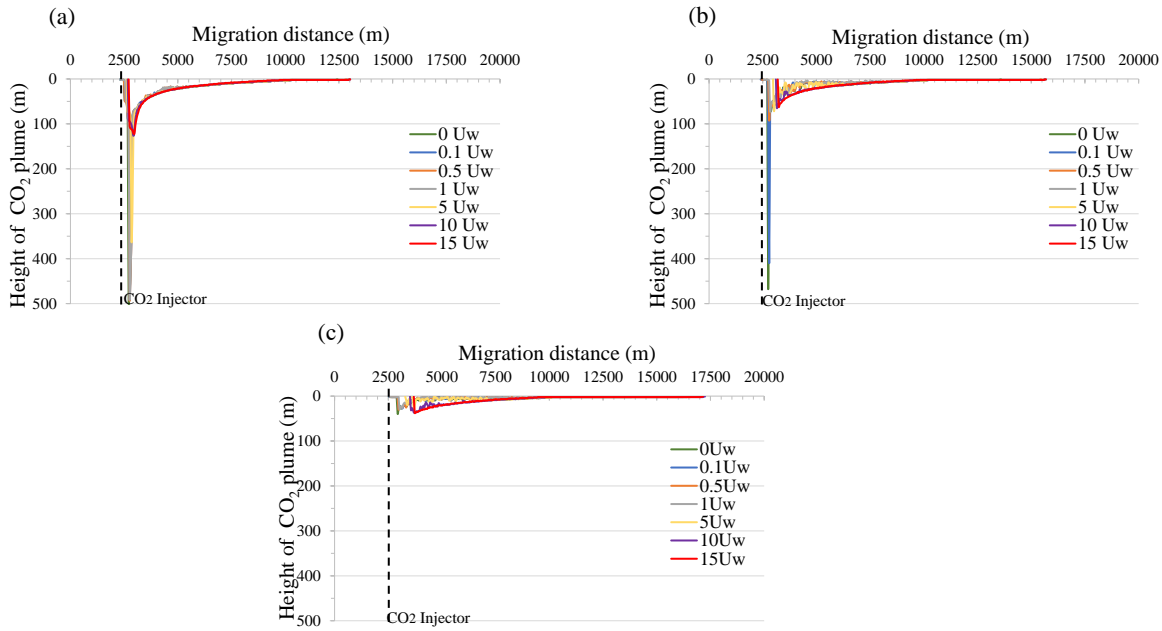


Fig. 7. The height of the plume and migration distance at various background water velocities after (a) 40 years, (b) 80 years and (c) 120 years of simulation time.

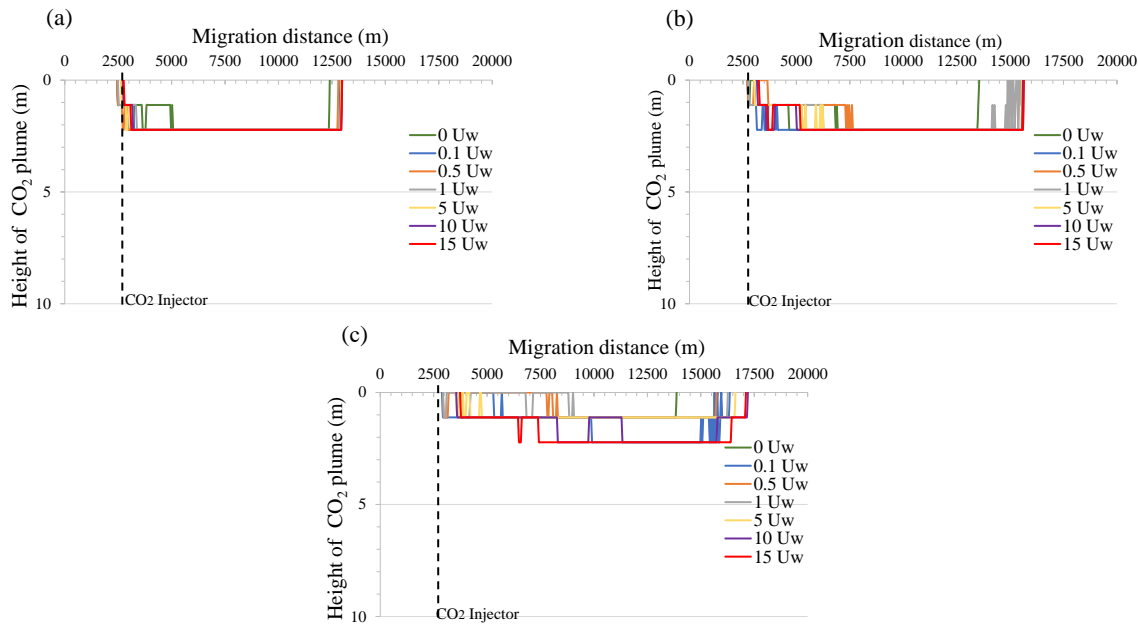


Fig. 8. Influence of background water velocity on the mobile CO₂ distribution after (a) 40 years, (b) 80 years and (c) 120 years of simulation.

for various background water velocities. The velocity of the plume decreases; however, the velocity of groundwater can have a substantial impact on the time it takes for the plume to come to a stop.

The plume velocity pattern during its late migration can be variable as background flow greatly impacts the spread of the mobile CO₂ and its dissolution. Darcy’s law is considered, which has a fundamental role in governing the movement of the CO₂ plume in the porous medium (Juanes and MacMinn, 2008), in order to analyse the relationship between

the plume migration and the background flow velocity:

$$u_i = \frac{kk_{ri}}{\mu_i} (\Delta P_i - \rho_i gh) \quad (1)$$

where u_i is the velocity of the gas phase, k is the absolute permeability, k_{ri} is the gas relative permeability, μ_i is the viscosity of the gas phase, ΔP_i is the change in pressure of the gas phase, ρ_i is the density of the gas, g is the gravitational acceleration, and h is the height of the mobile CO₂ column.

The velocity of the leading tip is analysed in terms of

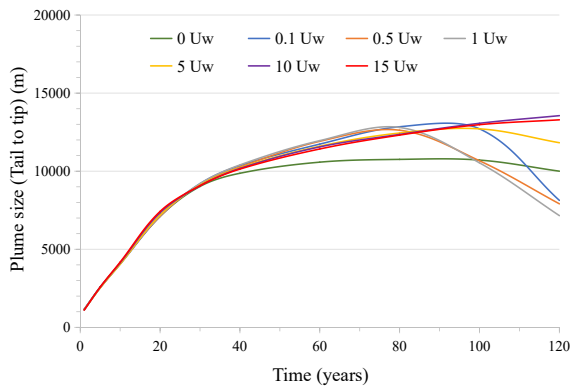


Fig. 9. The mobile CO₂ size at different velocities of background water flow.

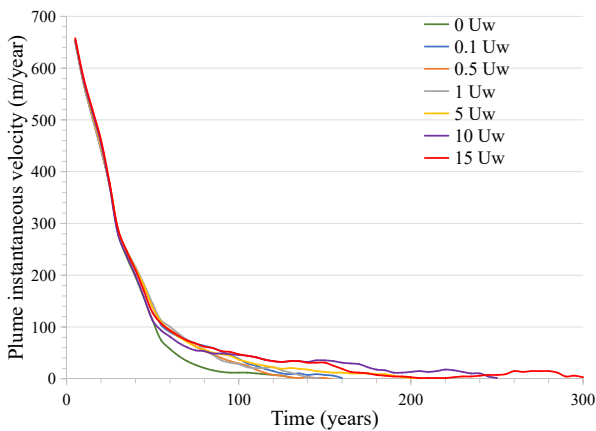


Fig. 10. Instantaneous velocity of the evolving plume at various background water velocities.

changing the plume height (h). The plume height in this part of the study is calculated from the point of contact between the leading tip of the plume with the caprock to the deepest part of the plume within the storage complex, measured as a vertical depth difference. Fig. 11 presents the change in the plume height with time for different background water flow velocities. The evolving plume enlarges with time and with increasing the water flow velocity, until it reaches a maximum, before it becomes completely trapped.

3.4 The effect of background water on the long-term fate of the CO₂

The influence of background water is further investigated on the dissolution of the injected CO₂, the long-term fate of the injected CO₂ and the dissolved CO₂ distribution in the storage formation. Fig. 12 shows the CO₂ dissolution profiles after 120 years of simulation time for background flow velocities of 1, 5 and 15 Uw. The stronger the flow, the greater the amount of CO₂ dissolved at the down-dip side of the plume and the further the dissolved CO₂ is removed away from the injection well. However, the profiles of CO₂ inventory at low (1 Uw) and at high (15 Uw) background water flow velocities during and after termination of injection, shown in Fig. 13, indicate

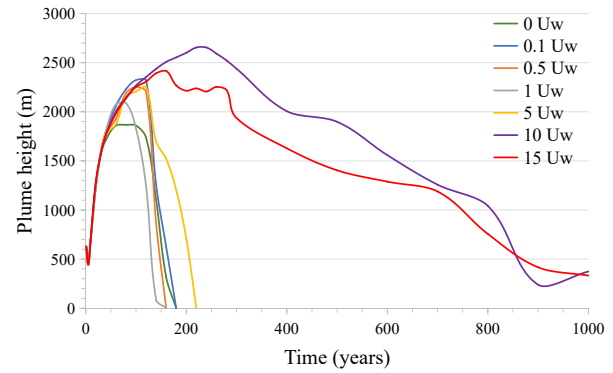


Fig. 11. The change in the mobile plume height for various background water velocities.

that in the late post-injection phase, the dissolution of CO₂ in water decreases with decreasing flow.

Fig. 14 illustrates the ultimate distribution of the dissolved CO₂ in water after 1,000 years of simulation for flow velocities of 1, 5 and 15 Uw. The results suggest that the background flow not only affects the CO₂ plume migration and dissolution process, but can also have a huge impact on the long-term movement of the CO₂-saturated water within the storage complex.

4. Discussion

As illustrated in the previous results, the groundwater flow velocity has a great effect on the CO₂ distribution and extent in the storage during the late post-injection period. Fig. 7 shows that increasing the background flow velocity significantly reduces the plume height near the injector and increases its extent with time. In addition, regardless of the speed with which the water flows, the plume leading edge migrates up dip over time. The difference in plume tip migration between 40 and 120 years can reach over 4 km for a groundwater velocity of 15 Uw. However, from these profiles, the impact of groundwater flow is more apparent at the lower end of the plume on the down-dip side of the aquifer, whereby the plume diminishes and travels further away from the injection well when the background velocity increases. This is because of the solubility of the residual CO₂ in water at the lower portion of the plume at later times, as fresh unsaturated water comes in contact with the residually trapped CO₂ first. This can be also confirmed from Figs. 4 and 5, where it can be noticed that the residual CO₂ around the injector (the yellow portion of the plume in these plots) becomes depleted over time. The height difference in the plume for the different water flow velocities is controlled by the instabilities caused by the convective dissolution of CO₂ in water (represented by the trend fluctuations in these plots) which is discussed below.

Comparison of the results shown in Fig. 8 indicates that, regardless of the velocity of groundwater, the height of the mobile CO₂ decreased at a slow rate over time. This is because the unsaturated groundwater flow is acting on the entire plume, and in order to dissolve the mobile CO₂ in the plume; it must first come into contact with the residual gas and remove that CO₂ by dissolution. Once the water flow dissolves most, if

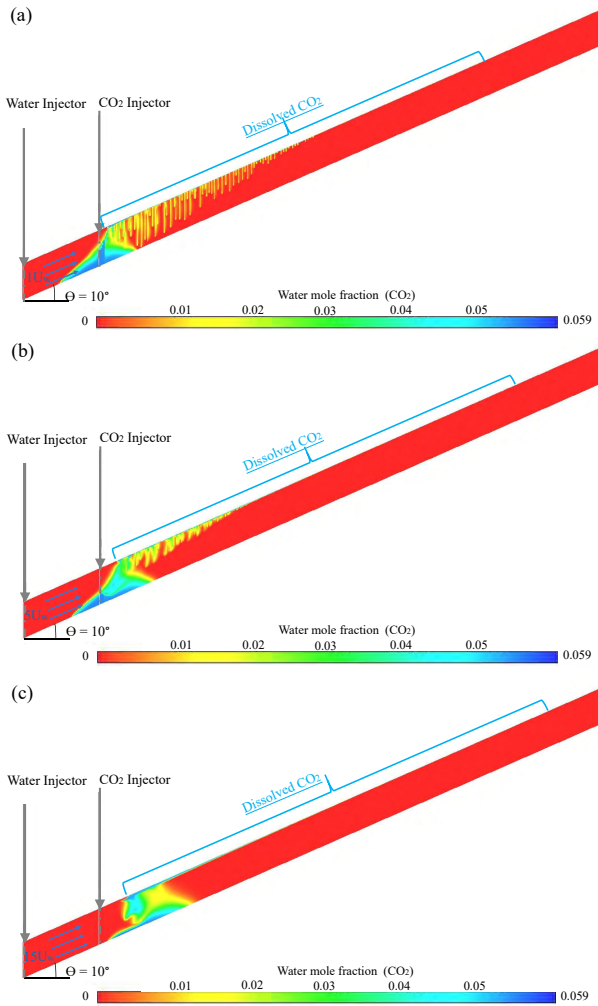


Fig. 12. Snapshots of CO₂ plume dissolution profiles after 120 years of simulation, for water flow velocities of (a) 1 Uw, (b) 5 Uw and (c) 15 Uw.

not all, the residually trapped CO₂, convective dissolution of the mobile CO₂ then becomes more dominant, especially at the lower portion of the mobile plume. As shown in Fig. 8, the height distribution of the mobile plume at its lower end becomes fragmented with time. The effect of convective dissolution expands and becomes apparent with time along the entire free phase CO₂-water interface (Fig. 8). The impact of background water flow over the long-term seems to be more significant at slower groundwater flow velocities. As can be observed from Fig. 8, the height of the mobile CO₂ reduces with time more so at slow flow velocities than at high flow velocities. This can be verified by the fragmentation intensity of the mobile CO₂ plume at different distances along the aquifer domain, which is caused by increasing the convective mixing at the CO₂-water interface and the quantum nature of the water velocities set in this sensitivity study.

Furthermore, the results in Fig. 9 show a non-monotonic behaviour of the size of the mobile CO₂ with water flow rate. This is because during the late period, the plume evolution is greatly affected by the physics of convective mixing, which according to the prior results shown in Fig. 6, varies with gro-

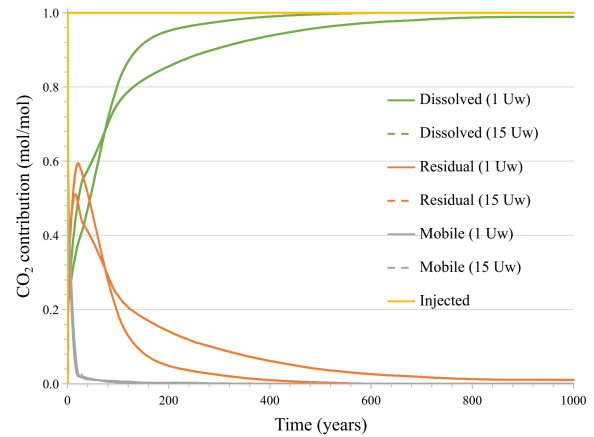


Fig. 13. Comparison of the fate of CO₂ at low and high background water velocities, 1 and 15 Uw, respectively. The vertical axis indicates the amount of CO₂ in each category in the inventory, normalised relative to the total volume of CO₂.

undwater flow velocity and time. This in turn affects the measurements of the continuous length of the mobile CO₂ that is not fragmented. Overall, regardless of the velocity of the flow, the mobile plume gradually enlarges with time due to its leading tip travelling quicker than its trailing end. This is predominantly due to increasing the buoyancy force, which was discussed in a previous study on the impact of background flow on the early post injection migration of the plume (Awag et al., 2023). This rises the potential risk of the CO₂ plume reaching a spillage point, such as leaky wells and fractures or faults, within the storage area during its displacement.

However, based on the results shown in Fig. 8, the height distribution of the mobile CO₂ varies between 1 and 2 m at low and high velocities, respectively, after 120 years of the plume migration. This means that the less mobile CO₂ stays in the aquifer, because the remaining injected plume is mainly retarded by convective dissolution in its late post-injection migration, which is further effective at lower flow velocities. This accordingly can reduce the potential risks associated with upwards CO₂ leakage during the late post-injection period.

Regardless of the background flow, as shown in Fig. 10, during the post-injection migration, the plume initially shows a great deceleration with time, which occurs, as explained in our previous analysis (Awag et al., 2023), owing to gravity and the large removal of the mobile CO₂ at the trailing edge by residual trapping. To support this discussion, the measurement of the height of the mobile CO₂ during its expansion is considered, as shown in Fig. 11. The plume height initially reduces during the first 8 years: this is during the plume vertical migration to the top boundary, and thus its velocity decreases significantly with time.

Fig. 10 shows that, irrespective of the velocity of background water, the plume over the longer-term continues to decelerate, but at a slower rate. This is because as the plume migrates, its height increases considerably with time, and the plume accelerates to some extent. This is also confirmed in the previous study of the early post-injection migration of the plume. Since the calculations in Fig. 10 are made for every 5

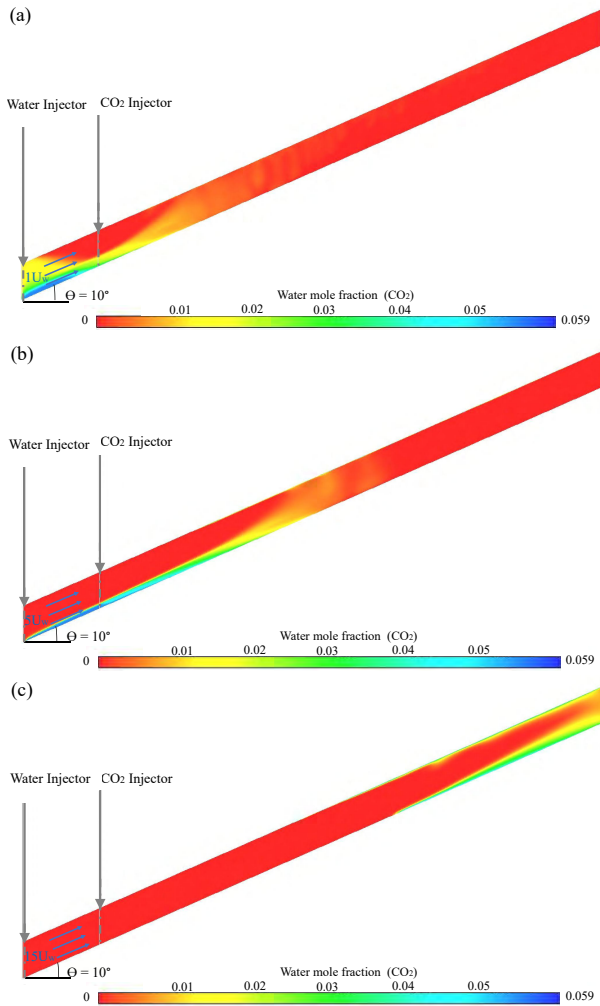


Fig. 14. Ultimate distribution of dissolved CO₂ after 1,000 years of simulation, for water flow velocities of (a) 1 Uw, (b) 5 Uw and (c) 15 Uw.

years of the CO₂ migration, the acceleration cannot be distinguished.

After almost 30 years of migration the background flow contributes to the impact of the buoyancy force and becomes more significant. As shown in Fig. 11, the development of convective flow patterns causes fluctuations in the measurements of the plume height. Since the convective dissolution of CO₂ in water is the predominant mechanism in reducing the mobile CO₂ during its late migration, it hinders the plume migration. The results shown in Fig. 10 indicate that, as the plume expands, its velocity will continue to decrease until it reaches a point where the plume starts to migrate with a constant velocity. This is the time when the plume reaches its maximum height. However, the intensity of the background flow can cause the plume to migrate further as it stretches, before it becomes completely exhausted by dissolution trapping. It is evident from Fig. 10 that the greater the flow velocity, the longer the time it takes for the plume to halt. Comparison of the results obtained in Fig. 10 with that of Fig. 11 indicate that, at slow flow velocity (1 Uw) the plume velocity converges to zero by 150 years, while at stronger flow velocity (15 Uw) the

plume comes to stop after 295 years that is when the plume height starts to significantly decrease to reach its minimum.

Considering the effect that background flow can have on CO₂ dissolution in water, Fig. 12 shows that increasing the velocity of background flow increases the dissolution of the residually trapped CO₂ at the trailing edge and removal of the CO₂-saturated water up-dip away from the injection point. However, comparison of the inventory profiles shown in Fig. 13 implies that the lower the velocity of the background flow, the greater the CO₂ dissolution in water and greater the amount of residually trapped CO₂. The mobile and residual CO₂ take longer time to completely dissolve in water with stronger flow rates. The strong background flow (15 Uw), Fig. 12, creates a clear zone around the injection well and relatively thick finger of CO₂-rich water, at the lower side of the plume, that is forced up-dip by the flow. Although this thick CO₂-rich water finger is continuously exposed to unsaturated water at high rates, the dissolution process is rather slow (confirmed in Fig. 13), since there is not enough time for the convective mixing to occur, which is essential to stimulate the rate of dissolution. By contrast, the CO₂ dissolution in the presence of low and intermediate background flows (1 and 5 Uw), Fig. 12, is comparatively fast. Where the thin convective fingers evolve within the plume, they allow for further dissolution as they are displaced downwards by the flow.

The above discussion is in contrast to the experimental results obtained by Michel-Meyer et al. (2017), where they found that the background flow affects the development of the convective flow patterns, but does not impact the rate of dissolution. This is also in contrast to the findings obtained from Awag et al. (2022), which demonstrate that in the early plume migration, the CO₂ dissolution in water increases with the flow velocity. This is because during the early post-injection period, the dissolution process is limited to the molecular diffusion of the buoyant CO₂ into the water at the interface. At that stage, the dissolution is enhanced because the strong background flow transports the buoyant CO₂ over great distances, increasing its contact surface area with the water at the interface. However, during the late post-injection migration the background flow may transport the dissolved CO₂ layer with the flow for long time, delaying the time it takes for convective flow patterns to develop and for the dissolved CO₂ to sink downwards. The presence and migration of the CO₂-saturated layer between the two currents as a result hinders the dissolution as it slows down the contact between the fresh water and the CO₂ currents (as shown in Figs. 12 and 13).

The eventual distribution of the trapped CO₂ shown in Fig. 14 signifies the influence that water flow rate has on the accumulated dense CO₂-saturated water at the bottom of the aquifer. At low background flow (1 Uw), the dissolved CO₂ slumps and accumulates at the bottom down-dip boundary of the aquifer; however, a distribution of water with a low fraction of dissolved CO₂ may also exist down-dip beneath the caprock. This implies the potential of CO₂ leakage if the water containing dissolved CO₂ penetrates the caprock. However, the greatest groundwater flow (15 Uw) displaces the denser water containing dissolved CO₂ to the up-dip boundary of the aquifer (this can be noticed beneath the caprock, where

dissolution is still progressing, and along the bottom of the aquifer, where water is fully saturated with CO₂). Although after 1,000 years of simulation there was no mobile CO₂ migration along the top of the aquifer, there is a greater likelihood of dissolved CO₂ displacement with water flow and subsequent migration to the surface if it reaches a spill point or the boundary. At intermediate water velocity (5 U_w), the denser CO₂-saturated water spreads at the bottom of the aquifer with a fair distribution along the down-dip and up-dip sides of the aquifer. This suggests the existence of a critical (perhaps optimal) groundwater flow velocity for dissolution trapping at which the CO₂-saturated water remains at the bottom of the aquifer with no further migration.

5. Conclusions

The following conclusions are drawn from this work.

- 1) The updip flow of unsaturated water removes, by dissolution, first the residual CO₂ before it can then interact with the mobile CO₂. Thereafter, the convective mixing at the mobile CO₂ and water interface becomes more dominant, reducing the height of the mobile CO₂ plume gradually with time. The background water flow velocity also has a great impact on the measurement of the mobile plume size, as it becomes fragmented with time due to the contribution of the convective dissolution, which is influenced by the flow strength.
- 2) The plume firstly decelerates significantly, during the vertical rise of the plume as it detaches from the well, because as a consequence its thickness reduces and water imbibition below the rising plume causes residual trapping at the trailing edge of the plume. Thereafter, the plume height increases as the plume lengthens with time, which reduces the rate at which the plume continues to decelerate. However, for stronger background flow, the plume migrates further as it stretches more before it comes to a stop. Once the plume reaches its maximum height, it migrates with a constant velocity.
- 3) The background flow effect becomes more dominant in reducing the volume of mobile CO₂ during the late migration of the plume. However, the greater the flow velocity, the longer it takes for the plume to become completely dissolved in water. This is because increasing the intensity of the flow does not allow enough time for the convective mixing to develop, which is essential in stimulating the dissolution process. The background flow can transport the dissolved CO₂ layer between the CO₂ and water for a long time, slowing down the interaction between the unsaturated water and CO₂ at the interface, which hinders the progression of dissolution.
- 4) The background water flow can have a significant effect on the long-term migration of the CO₂-saturated water within the storage complex. The eventual distributions of dissolved CO₂ with very weak and strong background flows impact the tendency of the dissolved CO₂ to persist underneath the caprock. This impacts the potential for dissolved CO₂ to migrate back to the surface should it encounter fractures or faults, or improperly completed

or abandoned wells. However, our results suggest the existence of a critical background flow velocity which can control the dissolved CO₂ and distribute it at the bottom of the aquifer, further away from the caprock.

Acknowledgements

The Libyan government are thanked for sponsoring Mawda Awag studies. CMG are thanked for providing use with the CMG-GEM software to use in this study. Energi Simulation are thanked for supporting the Chair in CCUS and Reactive Flow Simulation held by Eric Mackay.

Conflict of interest

The authors declare no competing interest.

Open Access This article is distributed under the terms and conditions of the Creative Commons Attribution (CC BY-NC-ND) license, which permits unrestricted use, distribution, and reproduction in any medium, provided the original work is properly cited.

References

- Awag, M., Mackay, E., Ghanbari, S. CO₂ plume migration in tilted aquifers subject to groundwater flow. Paper Presented at 83rd EAGE Annual Conference and Exhibition, Madrid, Spain, 1-5 June, 2022.
- Awag, M., Mackay, E., Ghanbari, S. The impact of background water flow on the early migration of a CO₂ plume in a tilted aquifer during the post-injection period. *Advances in Geo-Energy Research*, 2023, 9(2): 125-135.
- Awag, M., Mackay, E., Ghanbari, S. Numerical analysis on the direction of groundwater flux effects on the early post-injection migration of a CO₂ plume. *Carbon Capture Science & Technology*, 2024a, 10: 100153.
- Awag, M., Mackay, E., Ghanbari, S. Comparison between downdip and updip groundwater flow on early CO₂ migration in dipping storage aquifers. *Gas Science and Engineering*, 2024b, 121: 205181.
- Bachu, S. Review of CO₂ storage efficiency in deep saline aquifers. *International Journal of Greenhouse Gas Control*, 2015, 40: 188-202.
- Bachu, S., Gunter, W., Perkins, E. Aquifer disposal of CO₂: Hydrodynamic and mineral trapping. *Energy Conversion and Management*, 1994, 35(4): 269-279.
- Birkholzer, J. T., Oldenburg, C. M., Zhou, Q. CO₂ migration and pressure evolution in deep saline aquifers. *International Journal of Greenhouse Gas Control*, 2008, 40: 203-220.
- Cameron, D. A., Durlofsky, L. J. Optimization of well placement, CO₂ injection rates, and brine cycling for geological carbon sequestration. *International Journal of Greenhouse Gas Control*, 2012, 10: 100-112.
- CMG-GEM. Computer Modelling Group. s.l. 2022.
- Elenius, M., Voskov, D., Tchelepi, H. Interactions between gravity currents and convective dissolution. *Advances in Water Resources*, 2015, 83: 77-88.
- Emami-Meybodi, H., Hassanzadeh, H. Two-phase convective mixing under a buoyant plume of CO₂ in deep saline aquifers. *Advances in Water Resources*, 2015, 76: 55-71.

- Emami-Meybodi, H., Hassanzadeh, H., Ennis-King, J. CO₂ dissolution in the presence of background flow of deep saline aquifers. *Water Resources Research*, 2015, 51(4): 2595-2615.
- Ennis-King, J., Paterson, L. Role of convective mixing in the long-term storage of carbon dioxide in deep saline formations. *SPE Journal*, 2005, 10(3): 349-356.
- Förster, A., Norden, B., Zinck-Jørgensen, K., et al. Baseline characterization of the CO₂SINK geological storage site at Ketzin, Germany. *Environmental Geosciences*, 2006, 13(3): 145-161.
- Gunter, W., Wiwchar, B., Perkins, E. Aquifer disposal of CO₂-rich greenhouse gases: Extension of the time scale of experiment for CO₂-sequestering reactions by geochemical modelling. *Mineralogy and Petrology*, 1997, 59: 121-140.
- Han, W. S., Kim, K. Y. Evaluation of CO₂ plume migration and storage under dip and sinusoidal structures in geologic formation. *Journal of Petroleum Science and Engineering*, 2018, 169: 760-771.
- Han, W. S., Kue-Young, K., Esser, R. P., et al. Sensitivity study of simulation parameters controlling CO₂ trapping mechanisms in saline formations. *Transport in Porous Media*, 2011, 90: 807-829.
- Harter, T. Basic concepts of groundwater hydrology. California, University of California, 2003.
- Harvey, A. H. Semiempirical correlation for Henry's constants over large temperature ranges. *AIChE Journal*, 1996, 42(5): 1491-1494.
- Hassanzadeh, H., Pooladi-Darvish, M., Keith, D. The effect of natural flow of aquifers and associated dispersion on the onset of buoyancy-driven convection in a saturated porous medium. *AIChE Journal*, 2009, 55(2): 475-485.
- Hovorka, S. D., Benson, S. M., Doughty, C., et al. Measuring permanence of CO₂ storage in saline formations: The Frio experiment. *Environmental Geosciences*, 2006, 13(2): 105-121.
- Jossi, J. A., Stiel, L. I., Thodos, G. The viscosity of pure substances in the dense gaseous and liquid phase. *AIChE Journal*, 1962, 8(1): 59-63.
- Juanes, R., MacMinn, C. W. Upscaling of capillary trapping under gravity override: Application to CO₂ sequestration in Aquifers. Paper SPE 113496 Presented at SPE Symposium on Improved Oil Recovery, Tulsa, Oklahoma, 20-23 April, 2008.
- Juanes, R., MacMinn, C. W., Szulczewski, M. L. The footprint of the CO₂ plume during carbon dioxide storage in saline aquifers: Storage efficiency for capillary trapping at the basin scale. *Transport in Porous Media*, 2009, 82(1): 19-30.
- Kestin, J., Khalifa, H. E., Correia, R. J. Tables of the dynamic and kinematic viscosity of aqueous NaCl solutions in the temperature range 20-150 °C and the pressure range 0.1-35 MPa. *Journal of Physical and Chemical Reference Data*, 1981, 10(1): 71-88.
- Kumar, A., Noh, M. H., Ozah, R., et al. Reservoir simulation of CO₂ storage in deep saline aquifers. *SPE Journal*, 2005, 10(3): 336-348.
- Land, C. E. Calculation of imbibition relative permeability for two- and three-phase flow from rock properties. *SPE Journal*, 1968, 8(2): 149-156.
- Leonenko, Y., Keith, D. W. Reservoir engineering to accelerate the dissolution of CO₂ stored in aquifers. *Environmental Science & Technology*, 2008, 42(8): 2742-2747.
- Li, Y. K., Nghiem, L. X. Phase equilibria of oil, gas and water/brine mixtures from a cubic equation of state and Henry's Law. *The Canadian Journal of Chemical Engineering*, 1986, 64(3): 486-496.
- Mackay, E. J. Modelling the injectivity, migration and trapping of CO₂ in carbon capture and storage (CCS). in *Geological Storage of Carbon Dioxide (CO₂)*, edited by J. Gluyas and S. Mathias, Elsevier, Amsterdam, 2013, pp. 45-70.
- MacMinn, C., Szulczewski, M., Juanes, R. CO₂ migration in saline aquifers. Part 1. Capillary trapping under slope and groundwater flow. *Journal of Fluid Mechanics*, 2010, 662: 329-351.
- Michel-Meyer, I., Shavit, U., Rosenzweig, R. The role of water flow and dispersion in the dissolution of CO₂ in deep saline aquifers. *Energy Procedia*, 2017, 114: 4994-5006.
- Nghiem, L., Shrivastava, V., Kohse, B., et al. Simulation and optimization of trapping processes for CO₂ storage in saline aquifers. *Journal of Canadian Petroleum Technology*, 2010, 49(8): 15-22.
- Nicot, J. P. Evaluation of large-scale CO₂ storage on freshwater sections of aquifers: An example from the Texas Gulf Coast Basin. *International Journal of Greenhouse Gas Control*, 2008, 2(4): 583-593.
- Oh, J., Kim, K., Han, W., et al. Transport of CO₂ in heterogeneous porous media: Spatio-temporal variation of trapping mechanisms. *International Journal of Greenhouse Gas Control*, 2017, 57: 52-62.
- Peng, D. Y., Robinson, D. B. A new two-constant equation of state. *Industrial & Engineering Chemistry Fundamentals*, 1976, 15(1): 59-64.
- Pruess, K., Nordbotten, J. Numerical simulation studies of the long-term evolution of a CO₂ plume in a saline aquifer with a sloping caprock. *Transport in Porous Media*, 2011, 90: 135-151.
- Riaz, A., Cinar, Y. Carbon dioxide sequestration in saline formations: Part I-Review of the modeling of solubility trapping. *Journal of Petroleum Science and Engineering*, 2014, 124: 367-380.
- Rowe, A. M., Chou, J. C. Pressure-volume-temperature-concentration relation of aqueous sodium chloride solutions. *Journal of Chemical and Engineering Data*, 1970, 15(1): 61-66.
- Wang, F., Jing, J., Xu, T., et al. Impacts of stratum dip angle on CO₂ Geological storage amount and security. *Greenhouse Gases: Science and Technology*, 2016, 6(5): 682-694.